Flow Interactions During Axisymmetric Spinup

S. Ibrani* and H. Dwyer†
University of California, Davis, California

The purpose of this research study is to help understand the nature of the fluid mechanical processes which occur during the spinup of a liquid in an axisymmetric container. In the present investigation both a sphere and a right-circular cylinder geometries have been studied in order to isolate the influences of geometry on the fundamental processes. It has been shown that the initial inertial oscillation in the vessel is independent of vessel geometry and is due to the initial transit of the fluid formed in the "endwall" Ekman layer. Other basic processes such as time-dependent separation and the turning of fluid particles by fluid of larger angular momentum have been observed and documented. The numerical solution of this time-dependent problem has been considerably improved with the use of a direct solver method of the lower/upper decomposition type to obtain the solution of the Poisson equation for the stream function.

Introduction

THE purpose of this paper is to develop an understanding of the flow interactions which occur during the axisymmetric spinup of a liquid in a rigid container. The fundamental source of these interactions is the viscous Ekman layer[1,2] that develops on the walls of a rigid vessel as the interior fluid is being spunup by the wall viscous stresses. The nature of the interaction of the wall Ekman layer and the fluid in the interior of the vessel is a strong function of vessel geometry, initial state of the interior fluid, and the amount of angular momentum that has accumulated in the vessel interior. It will be shown that these multiple sources of time-dependent fluid interactions are the cause of separated flow, free shear layer, and of a complicated turning of fluid particles which can cause serious difficulties when a numerical solution is being obtained.

The basic study that has been the starting point of the present investigation has been the relatively high Reynolds number calculations carried out by Kitchens.[1] In that investigation both spinup from rest and spinup from an initial state of solid body rotation have been studied for the axisymmetric case of a right circular cylinder. The study by Kitchens identified the overall features of this flow and also identified those flow regions where the flow separates or where the viscous shear layer leaves the wall. Also, because of the relatively long development time of the flow and the limited computational resources that were available, not all of the flow features were studied in detail and the influence of geometry was not investigated at all.

In the present investigation the basic flow interactions which occur during spinup will be studied in detail and the influence of geometric changes partially studied. The basic tool utilized will be computer graphics and the tracing of the Ekman layer endwall particles as they leave the endwall region. Four different types of interactions have been identified:

1) Fluid particle angular momentum overshooting during a geometric turning of the flow.

2) Turning of the Ekman layer due to the initial angular momentum distribution.

3) Oscillations and flow reversal due to the initial startup and transit of the Ekman layer fluid particles.

4) Turning of the Ekman layer particles due to accumulation of fluid particles with angular momentum.

A number of the above fluid interactions are closely related, but since they occur at different times in the spinup process they have been classified in the manner given above in the text.

Some numerical improvements have been utilized in the present investigation. The numerical method utilized represents a significant improvement over previous efforts. These improvements are:

1) Formulation of Navier-Stokes equations in generalized nonorthogonal coordinates.

2) Use of a direct solver for the stream function equation.

3) Use of an iterative sweeping method to improve the convergence of nonlinear and nonorthogonal terms.

4) Use of adaptive gridding methods to improve grid resolutions.

The first three techniques have lead to substantial improvements in efficiency and accuracy of solution, but the fourth, adaptive gridding, has not yet yielded significant improvement. The lack of improvement has been caused by the diffuse and complicated character of the flow structures which develop in this problem.

Basic Equation and Numerical Method

The flows which will be presented in this paper are axisymmetric and they are impulsively started from rest or impulsively increased from a state of solid body rotation. The basic equations used as the starting point for the study are

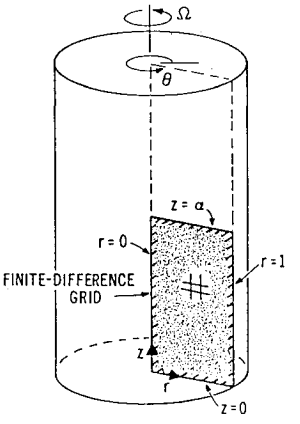

Fig. 1 Cylinder geometry for spinup calculation.

Presented as Paper 86-0036 at the AIAA 24th Aerospace Sciences Meeting, Reno, NV, Jan 6-9, 1986; received March 8, 1986; revision received Jan. 15, 1987. Copyright © American Institute of Aeronautics and Astronautics, Inc., 1987. All rights reserved.

*Research Associate, Department of Mechanical Engineering.
†Professor, Department of Mechanical Engineering.

the incompressible, unsteady, and laminar Navier-Stokes equations in the stream function (ψ), vorticity (ω), and circulation (γ) formulation. In vector form and in terms of cylindrical coordinates they are given as

$$\frac{\partial \boldsymbol{Q}}{\partial t}+\frac{\partial \boldsymbol{E}}{\partial r}+\frac{\partial \boldsymbol{F}}{\partial z}+\boldsymbol{G}=\frac{\partial \boldsymbol{R}}{\partial r}+\frac{\partial \boldsymbol{S}}{\partial z}+\boldsymbol{H}$$

where the column vectors are defined as

$$\boldsymbol{Q}=(r\omega,\gamma,0)^{-1}$$

$$\boldsymbol{E}=\left(\omega\frac{\partial\psi}{\partial z},\frac{\gamma}{r}\frac{\partial\psi}{\partial z},\frac{1}{r}\frac{\partial\psi}{\partial r}\right)^{-1}$$

$$\boldsymbol{F}=\left(-\omega\frac{\partial\psi}{\partial r},-\frac{\gamma}{r}\frac{\partial\psi}{\partial z},\frac{1}{r}\frac{\partial\psi}{\partial z}\right)^{-1}$$

$$\boldsymbol{G}=\left(-\frac{\omega}{r}\frac{\partial\psi}{\partial z}-\frac{2\gamma}{r^2}\frac{\partial\gamma}{\partial z},0,0\right)^{-1}$$

$$\boldsymbol{R}=\nu\left(r\frac{\partial\omega}{\partial r},\frac{\partial\gamma}{\partial r},0\right)^{-1}$$

$$\boldsymbol{S}=\nu\left(r\frac{\partial\psi}{\partial z},\frac{\partial\gamma}{\partial z},0\right)^{-1}$$

$$\boldsymbol{H}=\nu\left(-\frac{\psi}{r},-\frac{1}{r}\frac{\partial\gamma}{\partial r},\omega\right)^{-1}$$

where r and z are the two cylindrical coordinates shown in Fig. 1, u and w the respective velocities along these coordinate directions, v the velocity in the spin direction, and ν the kinetic viscosity of the fluid. The relationship between the velocities and the new dependent variables are given as

$$\omega=\frac{\partial u}{\partial z}-\frac{\partial w}{\partial r}\qquad u=\frac{1}{r}\frac{\partial\psi}{\partial z}\qquad w=-\frac{1}{r}\frac{\partial\psi}{\partial r}\qquad \gamma=rv$$

In order to solve the more general problems in this paper, the equations were transformed to a conservative nonorthogonal form which allows for the use of generalized coordinate systems.[4] These transformed equations in terms of the transformed coordinates ξ, η, and τ are

$$\frac{\partial \boldsymbol{Q}}{\partial \tau}+\frac{\partial \boldsymbol{E}}{\partial \xi}+\frac{\partial \boldsymbol{F}}{\partial \eta}+\boldsymbol{G}=\nu\left(\frac{\partial \boldsymbol{R}}{\partial \xi}+\frac{\partial \boldsymbol{S}}{\partial \eta}+\boldsymbol{H}\right)$$

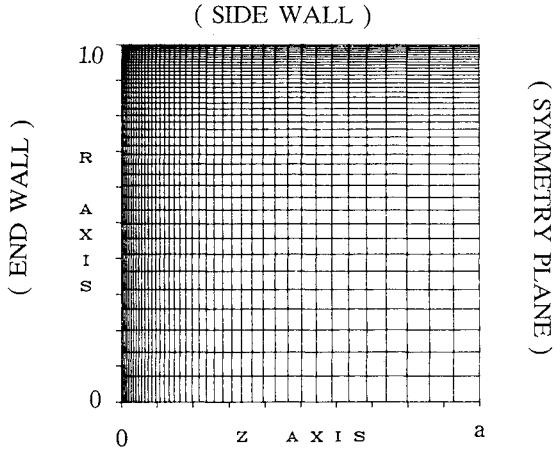

Fig. 2 Finite-difference grid cylinder.

where the new column vectors are given as

$$\boldsymbol{Q}=(r\omega/J,r\gamma/J,0)^{-1}$$

$$\boldsymbol{E}=(r\omega\xi_t/J-\omega\psi_g,r\gamma\xi_t/J-\gamma\psi_\eta,$$
$$J/r\psi_\xi[r_\eta^2+z_\eta^2]-\psi_\eta[r_\eta r_\xi+z_\eta z_\xi])^{-1}$$

$$\boldsymbol{F}=(r\omega\eta_t/J-\omega\psi_\xi,r\gamma\eta_t/J-\gamma\psi_\xi,$$
$$J/r\psi_\eta[r_\xi^2+r_\xi^2]-\psi_\xi[r_\eta r_\xi+z_\eta z_\xi])^{-1}$$

$$\boldsymbol{G}=(2\gamma/r^2[\gamma_\xi r_\eta-\gamma_\eta r_\xi]-\omega/r[\psi_\xi r_\eta-\psi_\eta r_\xi],0,0)^{-1}$$

$$\boldsymbol{R}=rJ(\omega_\xi[r_\eta^2+z_\eta^2]-\omega_\eta[r_\eta r_\xi+z_\eta z_\xi],$$
$$\gamma_\xi[r_\eta^2+z_\eta^2]-\gamma_\eta[r_\eta r_\xi+z_\eta z_\xi]+2\gamma z_\eta,0)^{-1}$$

$$\boldsymbol{S}=rJ(\omega_\eta[r_\xi^2+z_\xi^2]-\omega_\xi[r_\eta r_\xi+z_\eta z_\xi],$$
$$\omega_\eta[r_\xi^2+z_\xi^2]-\omega_\xi[r_\eta r_\xi+z_\eta z_\xi]-2\gamma z_\xi,0)^{-1}$$

$$\boldsymbol{H}=\nu(\omega/[rJ],0,\omega/J)^{-1}$$

and the Jacobian J is defined as $J=\xi_r\eta_z-\xi_z\eta_r$.

The numerical method employed to solve the equations consisted of a predictor/corrector sweeping method for the ω and γ equations and the use of a direct banded solver for the solution of the ψ equation. The iterative method consisted of an alternating direction predictor/corrector technique in the transformed plane with updating of variables and use of the previous sweep for the non-implicit direction and cross derivative terms. The technique has the option of being first or second order accurate in time (equivalent to fully implicit or Crank-Nicolson for a linear problem) and converges on the full nonlinear problem as the number of correctors are increased. The method also improves the treatment of the cross-derivative terms since these terms are also updated and are not treated in a purely explicit way as with most noniterative methods.

The direct banded solver was developed for a nine-point second-order finite-difference approximation and use was made of the numerical mathematical library LINPACK.[7] With this procedure a lower/upper decomposition of the banded matrix was performed, once for a given geometry and saved for a rapid back solve for the stream function. The technique has proven to be considerably faster than iterative techniques and removes all uncertainty concerning the convergence of the sensitive Poisson equation for the stream function. It is strongly felt that the direct solution for ψ is and will be the preferred method for two-dimensional problems. In a later section of the paper some preliminary results with the use of grid adaption will be described. These results have not been encouraging, and more research must be carried out.

Physical Problems and Results

The discussion of the results will be divided into three different flows which will illustrate the basic characteristics of the spinup process. The first flow will be that of a right circular cylinder while the second will be a spherical vessel. By comparing the different flow features of these two geometries, the nature of the Ekman layer will be clearly illustrated and a deeper understanding of the spinup process obtained. A typical grid geometry for a right-circular cylinder is shown in Fig. 2 where the axis of rotation is the z axis. The grid is expanded geometrically from both the endwall where the Ekman layer forms and from the sidewall where the Ekman layer is forced to flow. It is along both of these noslip walls where the thin, high-gradient boundary-layer regions are formed.

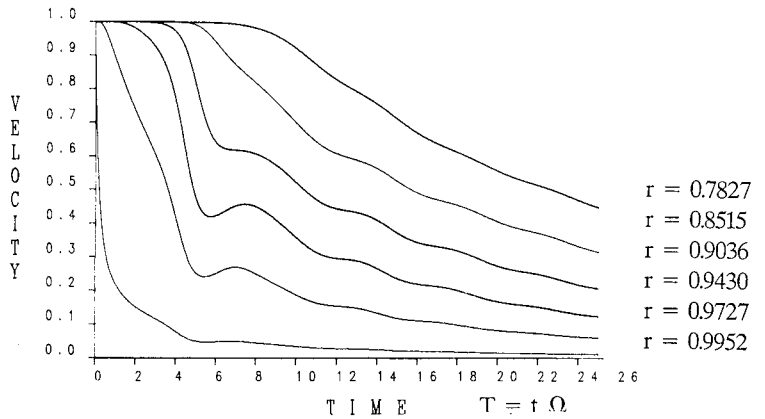

Fig. 3 Change of velocity $(1-V/r)$ for cylinder; $R=1$, $Z=0.3182$, $Re=7334$.

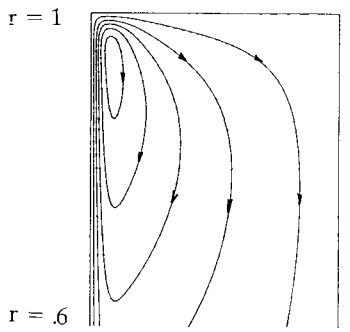

Fig. 4 Streamline pattern, $T=1.0$.

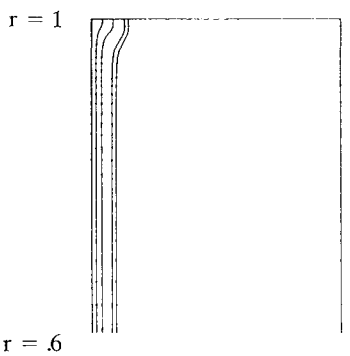

Fig. 5 Isotherm pattern, $T=1.0$; five isotherms 0.2 – 1.0.

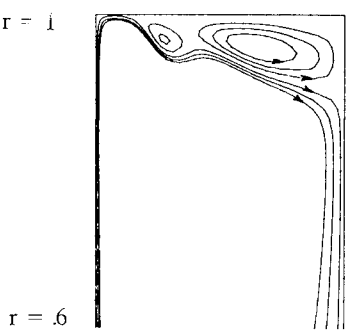

Fig. 6 Streamline pattern, $T=7.0$.

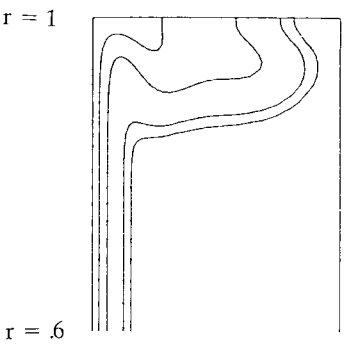

Fig. 7 Isotherm pattern, $T=7.0$.

In order to validate the program, the first calculation performed was identical to one carried out by Kitchen[1] where the ratio of the length of the sidewall a to the radius r was $a/r=0.3182$. For a spinup Reynolds number of $Re=\Omega r_0^2/\nu=7334$, a typical velocity spinup history at various locations along the axis of symmetry is shown in Fig. 3. The spinup velocity v has been presented so that it is zero when solid body rotation has been reached and one when the fluid is not spinning at all. The results in Fig. 3 are identical (Ref. 6 contained results that were in error) with Kitchens and they illustrate clearly the typical inertial oscillations which occur at high Reynolds number during the spinup process.

In order to determine the physical nature of these oscillations an "energy equation" was solved with a Prandtl number of one and no interaction with the fluid mechanics (passive scalar). The energy equation was given an initial condition of $T=0$ and the following boundary conditions:

$$\text{Endwall:} \quad T=1$$

$$\text{All other boundaries:} \quad \frac{\partial T}{\partial n}=0 \text{ (adiabatic)}$$

Therefore, the only way the temperature can increase is by being carried from the endwall Ekman layer into the interior of the vessel. At an early time in the spinup process ($T=1.0$), before the onset of inertial oscillations, the flow streamline pattern and temperature contours are shown in Figs. 4 and 5. It is clear from these temperature patterns that the Ekman layer is thin and that only a small amount of fluid has come out of the endwall.

The streamline patterns show clearly that the flow is moving globally, since a global pressure field is setup instantaneously in an incompressible fluid. However, the temperature contours show even more clearly that only a small amount of the moving fluid has come out of the sidewall Ekman layer. Therefore, even though the Ekman layer on the endwall is setup quickly, the rotational fluid particles existing from the endwall move relatively slowly.

The same type of plots of the streamlines and temperature contours at a time during the first inertial oscillation are shown in Figs. 6 and 7. It is clearly seen that time-dependent separated flow has developed and that the fluid particles emitted from the endwall Ekman layer have influenced the symmetry plane. With this information, a physical explanation of the inertial oscillations can be postulated. At early

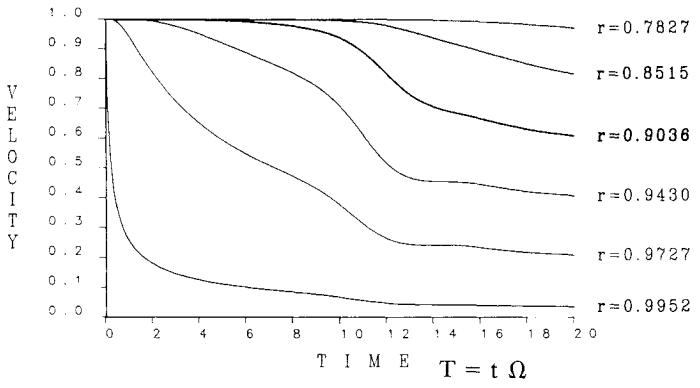

Fig. 8 Change of velocity $(1 - V/r)$ for cylinder; $R = 1$, $Z = 1$, $Re = 10^4$.

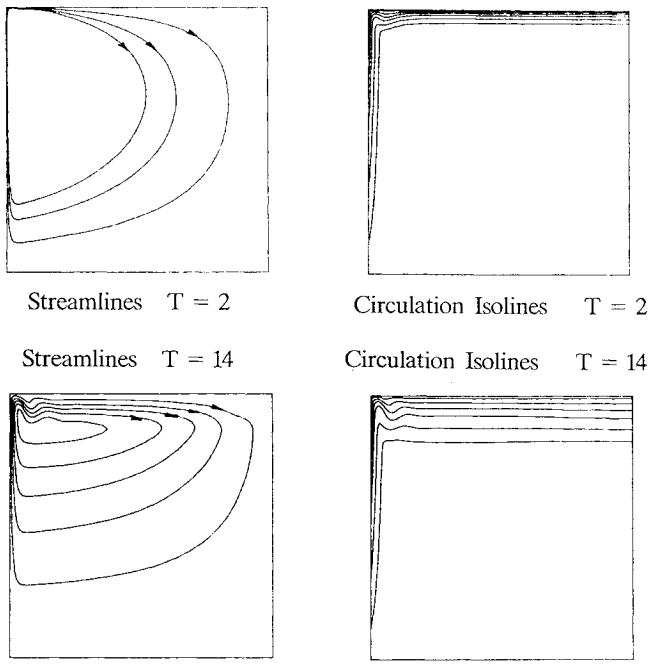

Fig. 9 Streamlines and distribution of circulation.

times in the spinup process the Ekman layer fluid turns at the end/sidewall junction and moves across the sidewall. When this rotating fluid reaches the symmetry plane it is again forced to turn and begins to move into the interior of the vessel. Since the fluid in the interior of the vessel is not rotating, a centrifugal pressure gradient is developed dynamically and this pressure gradient stops the rotating fluid from moving into the nonrotating fluid. As the fluid is stopped the particles move back toward the sidewall until they obtain enough support from the continually working endwall Ekman layer. Also, since the Reynolds number is high the entire process has a tendency to overshoot due to inertia.

The previous explanation describes the first inertial oscillation but does not give a completely clear description of the persistence shown in Fig. 3. These further oscillations are probably due to a coupling between the Ekman layer and the rotating fluid moving into the interior of the vessel and also the fact the fluid particles have obtained considerable angular momentum. This angular momentum can serve as a source of inertial oscillations as is well known for a fluid in solid body rotation (see Ref. 8).

If the description of the first inertial oscillation is correct, then the oscillation should be delayed when the sidewall length is increased. Figure 8 shows this effect for a cylindrical vessel with $a/r = 1.0$, and it is seen that the oscillations are also weaker, since the Ekman layer has the same strength for a much longer sidewall. Some other interesting features of this flow are given in Fig. 9 where the circulation and streamline patterns are shown for an early and first oscillation time. It is seen in both Figs. 6 and 9 that the streamline pattern oscillates in the flow corner which divides the end- and sidewall boundary layers. This oscillation was thought originally to be due to the corner itself[1,6] but another more general explanation can now be given. This other explanation came from the study of another spinup geometry—the sphere.

Shown in Figs 10–14 are the grid geometry and some flow characteristics of the spinup in a spherical vessel. A very significant feature of the spherical geometry is that the distinctioin between the end- and sidewalls has been lost, since the Ekman layer exists on the entire vessel wall. Rather than an abrupt turning at the corner, a continuous turning occurs until the plane of symmetry. The results in Figs. 10–14 show that the spherical spinup process has many similar features to the cylinder, but with some differences.

For two vessels of equivalent size, a (cylindrical geometry) $= R$ (spherical vessel), the spinup velocities v in Figs. 8 and 11 have similar characteristics, but with the sphere developing the first inertial oscillation at an earlier time. The sphere develops the oscillation earlier since the Ekman layer extends directly to the line of symmetry due to the turning of the wall. Therefore, rotating fluid is forced to move relatively more quickly into the interior of the vessel for the spherical geometry, and the resulting inertial oscillation occurs at an earlier time. It should be mentioned that the strength of the Ekman layer for the spherical geometry is effectively zero at the symmetry plane, and that the inertial oscillations result from the accumulation of Ekman layer fluid from radii below the symmetry plane.

The circulation and streamline patterns for the spherical geometry given in Figs. 12 and 14 show many of the characteristics of the cylinder. Figure 12 shows that rotating fluid with significant circulation has accumulated near the symmetry plane by the time the first inertial oscillation has occurred ($T = 8$). The streamline pattern in Fig. 12 exhibits the typical "separation" bubble that develops as the Ekman layer is forced to stop temporarily. As the Ekman layer resumes and continues to aid the spinup process, the flow retains a history of this separation bubble, as shown in Fig. 13.

An understanding of the process that occurs in the corner between the end- and sidewall on the cylinder can now be obtained by observing the distribution of circulation for both the cylinder and sphere. The circulation patterns in both Fig.

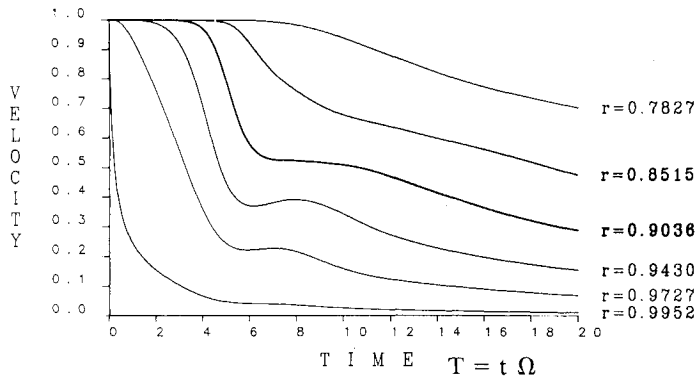

Fig. 10 Change of velocity $(1-V/r)$ for sphere; $R=1$, $Re=10^4$.

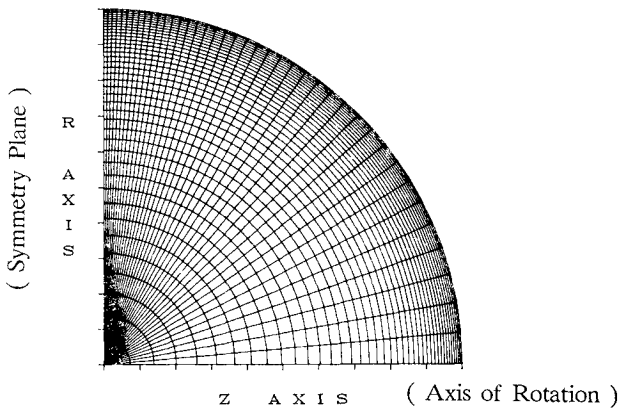

Fig. 11 Finite-difference grid sphere.

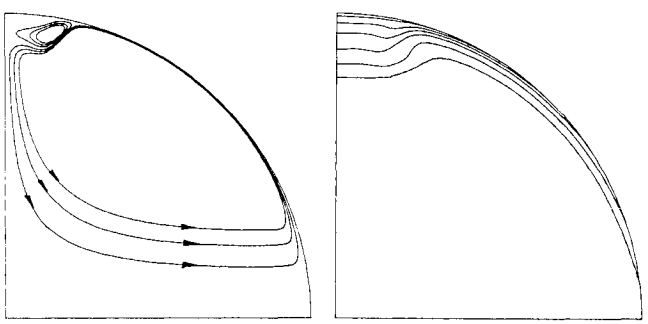

Fig. 12 Streamlines and distribution of circulation.

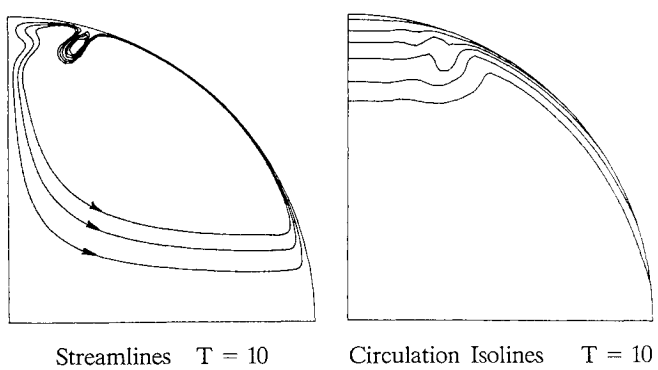

Fig. 13 Streamlines and distributin of circulation.

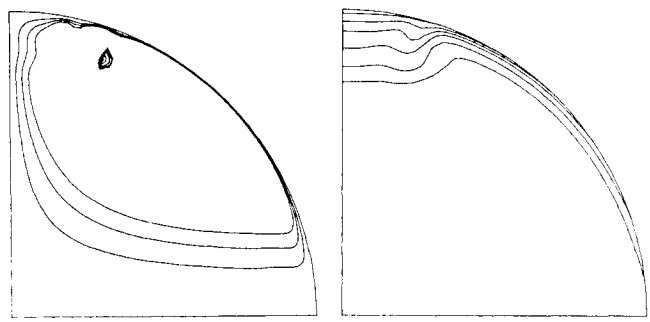

Fig. 14 Streamlines and distribution of circulation.

9, $T=14$, and Fig. 14, $T=16$, clearly show that there are spatial oscillations in the circulation for both geometries. The reason for these spatial oscillations is the inertial overshooting of the fluid coming out of the Ekman layer. For the cylindrical geometry the fluid particles come out of the Ekman layer at the corner junction, while for the sphere the exiting of fluid particles is more gradual. However, in both cases the Ekman layer particles are moving out to larger radius and for early times in the spinup process the fluid particles tend to overshoot their level of circulation on the sidewall or at the symmetry plane. This overshooting is a phenomenon that occurs during the entire spinup process and is independent of the time dependent inertial oscillations which are shown in Figs 3, 8, and 10. Also, additional calculations that have been carried out for other geometries show exactly the same behavior.

During later times in the spinup process for the spherical geometry another physical process also tends to cause waves in space. This physical process is the movement of particles of lower circulation around particles of higher circulation. For the spherical geometry there is a rapid accumulation of high circulation fluid at the symmetry plane. As particles of fluid with lower circulation are brought up by the Ekman layer, the local centrifugal pressure gradients cause the particles with lower circulation to move under the higher circulation particles. Therefore, the patterns in Figs. 12-14 can be explained by both overshooting and centrifugal turning.

To illustrate further these physical processes with another variation of the problem, some results will now be presented for partial spinup form an initial state of solid body rotation. With an initial state of solid body rotation there is the additional feature of existing circulation and centrifugal pressure gradients. For the case of a Reynolds number increase from 6000 to 25,000 the approach to a new state of solid body rotation is shown in Fig 15, while Figs. 16-18 give some typical corresponding circulation and streamline patterns. A comparison of Fig. 8 with Fig. 15 shows that the ap-

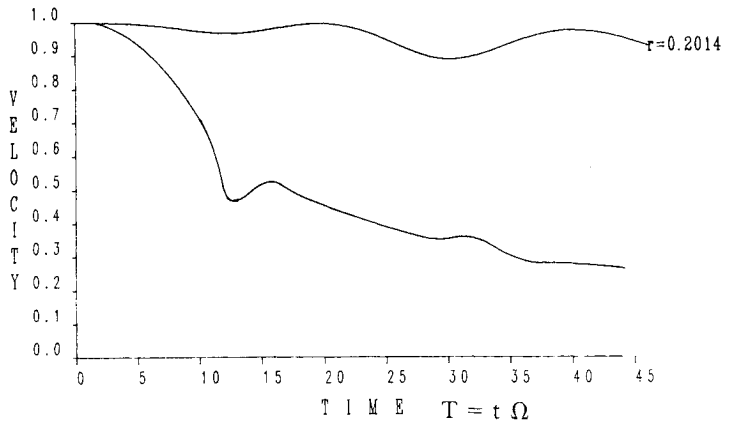

Fig. 15 Velocity $O_m(1-V/r)/(O_m-O_{mi})$ for cylinder; $R=1$, $Z=1$, $O_{mi}=O_m/4$, $Re=25*10^4$.

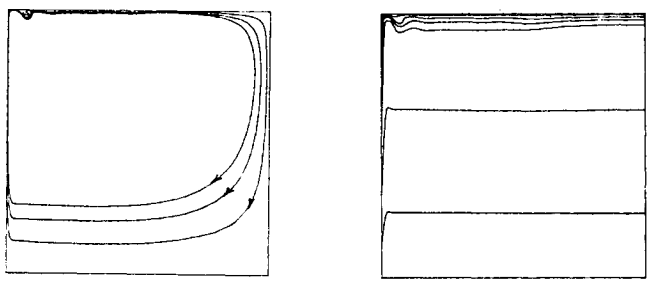

Streamlines T = 8 Circulation T = 8

Fig. 16 Streamlines and distribution of ciruclation.

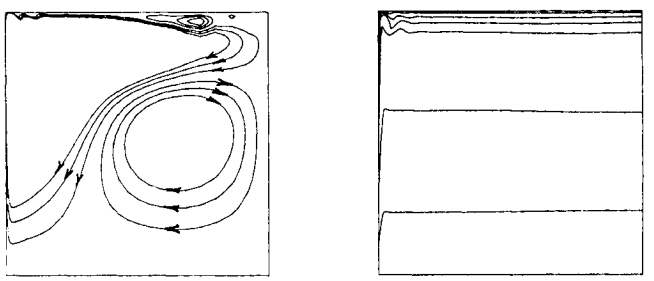

Streamlines T = 16 Circulation T = 16

Fig. 17 Streamlines and distribution of circulation.

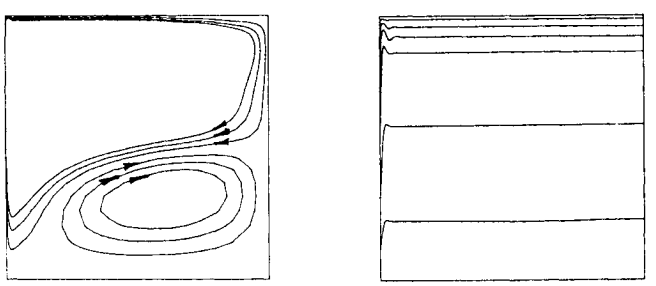

Streamlines T = 36 Circulation T = 36

Fig. 18 Streamlines and distribution of circulation.

pearance of the first inertial oscillation occurs at exactly the same time and thus scales with the length of the sidewall as mentioned previously.

The streamline and circulation patterns have similar characteristics to previous results, but the overshooting now occurs along the entire Ekman layer. The maximum overshoot still occurs near the corner between the end- and sidewalls, but some overshooting in circulation is observed for all the locations shown. The streamline patterns in Figs. 16 and 17 are typical of the early and first oscillation patterns of the full spinup case, but the pattern near the rotation axis are dramatically different. The closed streamline patterns shown in Figs. 17 and 18 are the result of fluid particles moving around particles with greater circulation. Due to the unsteady nature of the flow it should be remembered that pathlines are not streamlines as shown previously with the temperature contours. The streamline patterns for the partial spinup case is in general quite complicated because of the continuous process of fluid particle overshooting and trying to find their appropriate level of time dependent circulation.

Conclusions

A numerical study of the high Reynolds number axisymmetric spinup process in vessels of cylindrical and spherical shape has been carried out. The major conclusion gained from the investigation are the following:

1) The first inertial oscillation to appear in the cylindrical vessel is due to the accumulation of fluid with circulation at the symmetry plan and then stopping due to the lack of sufficient support from the Ekman layer. The exact time of the oscillation scales on the sidewall length of the vessel. For a spherical vessel the oscillations occur rather early during the spinup process since the Ekman layer endwall and sidewall lose their distinction. However, for both flows the motion of the fluid with circulation is stopped and does not penetrate into nonrotating fluid.

2) When the Ekman layer is turned by a sharp geometric corner or by fluid with a larger amount of circulation an overshooting in the spatial distribution of circulation occurs. This spatial oscillation is independent of vessel geometry and can occur at almost any location in the vessel.

3) As the Ekman layer fluid is dynamically stopped or turned by fluid with greater circulation "separation bubbles" form and disappear. The time-dependent streamlines can be misleading since for unsteady flows the differences between pathlines and streamlines can be large.

4) An efficient time-dependent numerical method has been developed and applied successfully to the Naver-Stokes equations. The method is of the predictor/corrector type and employs an ADI like sweeping technique for the time marching transport equations (ω and γ). A major advantage is that the nonlinear and cross derivative terms are updated and evaluated implicitly.

5) The Poisson equation relating the stream function to the vorticity has been solved by a direct method of the lower/upper decomposition type. The technique is accurate, efficient, and capable of treating complex non-orthogonal shapes. For time-dependent flows it is particularly attractive, since the matrix decomposition can be performed before the calculation is begun, and a backsolve is only required at all other times when the solution is required.

Acknowledgment

This research was supported by the U. S. Army Office of Scientific Research.

References

[1]Kitchens, C. W., "Navier-Stokes Solutions for Spin-Up from Rest in a Cylindrical Container," U.S. Army Ballistic Research Laboratory, Aberdeen Proving Ground, MD, Technical Rept. ARBL-TR-02193, Sept. 1979.

[2]Briley, W. R. and Walls, H. A., "A Numerical Study of Time-Dependent Rotating Flow in a Cylindrical Container at Low and Moderate Reynolds Numbers," *Proceedings of the 2nd International Conference on Numerical Methods in Fluid Dynamics, Lecture Notes in Physics*, Springer-Verlag, Vol. 8, 1970, pp. 377-384.

[3]Dwyer, H. A., "Grid Adaptation for Problems with Separation Cell Reynolds Number, Shock-Boundary Layer Interaction, and Accuracy," AIAA Paper 83-0449, Jan. 1983.

[4]Dwyer, H. A. and Sanders, B. R., "Droplet Heating and Vaporization at High Reynolds and Peclet Numbers," AIAA Paper 83-1706, July 1983.

[5]Peaceman, D. W. and Rockford, H. H. Jr., "The Numerical Solution of Parabolic and Elliptic Differential Equations," *J. SIAM*, Vol. 3, No. 1, 1955, pp. 28-41.

[6]Dwyer, H. A., "Calculation of Liquid Spin-Up in Cylindrical Vessels," AIAA Paper 84-0341, Jan. 1984.

[7]Dongarra, J. J. et al., *LINPACK-User's Guide SIAM*, Philadephia, 1979.

[8]Widemeyer, E. H., "The Unsteady Flow Within a Spinning Cylinder," *Journal of Fluid Mechanics*, Vol. 20, Part 3, 1964, pp. 383-399.